United States
Environmental Protection
Agency

EPA-600/R-05/088
August 2005

Measurement of Fugitive Emissions at a Landfill Practicing Leachate Recirculation and Air Injection

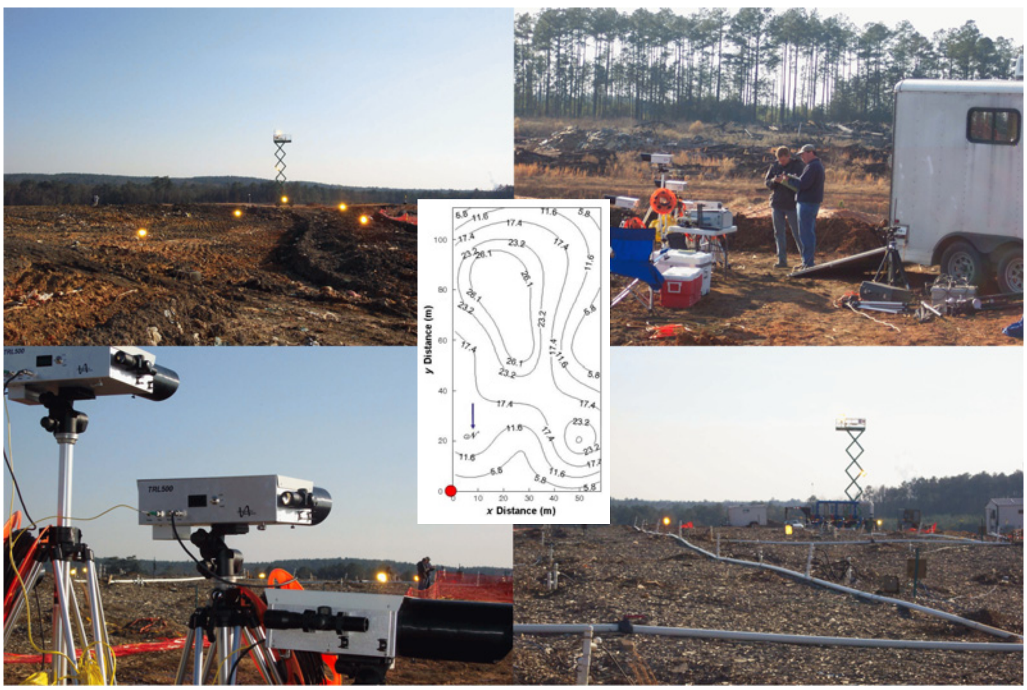

EPA-600/R-05/088
August 2005

Measurement of Fugitive Emissions at a Landfill Practicing Leachate Recirculation and Air Injection

by

Mark Modrak, Ram A. Hashmonay, Ravi Varma, and Robert Kagann
ARCADIS G&M, Inc
4915 Prospectus Dr. Suite F,
Durham, NC 27713

Contract Number: EP-C-04-023
Work Assignment Numbers 0-30 and 1-30

Project Officer: Susan Thorneloe
U.S. Environmental Protection Agency
National Risk Management Research Laboratory
Air Pollution Prevention and Control Division
Research Triangle Park, NC 27711

U.S. Environmental Protection Agency
Office of Research and Development
Washington, DC 20460

Abstract

Recently, research has begun on operating bioreactor landfills. The bioreactor process involves the injection of liquid into the waste mass to accelerate waste degradation. The EPA and ARCADIS conducted a fugitive emission characterization study at the Three Rivers Solid Waste Technology Center Landfill located near Jackson, South Carolina. The survey area is a two acre research and development site that practices leachate recirculation and air injection. The site is located within the Subtitle D Landfill.

The focus of this study is to evaluate emissions of fugitive gases, such as methane and hazardous air pollutants, at the site using scanning open-path Fourier transform infrared spectrometers and open-path tunable diode laser absorption spectroscopy. The study involved a technique developed through research funded by the EPA National Risk Management Research Laboratory, which uses ground-based optical remote sensing technology, known as radial plume mapping. The horizontal radial plume mapping (HRPM) method was used to map surface methane concentrations, and the vertical radial plume mapping (VRPM) method was used to measure emissions fluxes downwind of the site.

HRPM surveys detected the presence of a methane hot spot near the center of the site, with peak concentrations ranging from over 26 ppm to over 48 ppm above ambient background levels. An additional HRPM survey was conducted, at the request of the site operator, while leachate was being pumped from a small holding pond located in the southeast corner of the site to another small holding pond located in the northwest corner of the site. This survey detected an additional methane hot spot located near the northwest corner of the site with concentrations greater than 23 ppm above ambient background levels.

The results of the VRPM surveys found upwind methane flux values between 14 and 20 g/s, and downwind methane flux values between 10 and 18 g/s. The downwind methane flux values from 21 and 22 January 2004, are probably lower than the corresponding upwind values because the prevailing winds at the time of the surveys carried a large portion of the plume from the upwind hot spot outside of the downwind VRPM configurations.

Foreword

The U.S. Environmental Protection Agency (EPA) is charged by Congress with protecting the Nation's land, air, and water resources. Under a mandate of national environmental laws, the Agency strives to formulate and implement actions leading to a compatible balance between human activities and the ability of natural systems to support and nurture life. To meet this mandate, EPA's research program is providing data and technical support for solving environmental problems today and building a science knowledge base necessary to manage our ecological resources wisely, understand how pollutants affect our health, and prevent or reduce environmental risks in the future.

The National Risk Management Research Laboratory (NRMRL) is the Agency's center for investigation of technological and management approaches for preventing and reducing risks from pollution that threaten human health and the environment. The focus of the Laboratory's research program is on methods and their cost-effectiveness for prevention and control of pollution to air, land, water, and subsurface resources; protection of water quality in public water systems; remediation of contaminated sites, sediments and ground water; prevention and control of indoor air pollution; and restoration of ecosystems. NRMRL collaborates with both public and private sector partners to foster technologies that reduce the cost of compliance and to anticipate emerging problems. NRMRL's research provides solutions to environmental problems by: developing and promoting technologies that protect and improve the environment; advancing scientific and engineering information to support regulatory and policy decisions; and providing the technical support and information transfer to ensure implementation of environmental regulations and strategies at the national, state, and community levels.

This publication has been produced as part of the Laboratory's strategic long-term research plan. It is published and made available by EPA's Office of Research and Development to assist the user community and to link researchers with their clients.

Sally Gutierrez, Director
National Risk Management Research Laboratory

EPA Review Notice

This report has been peer and administratively reviewed by the U.S. Environmental Protection Agency and approved for publication. Mention of trade names or commercial products does not constitute endorsement or recommendation for use.

This document is available to the public through the National Technical Information Service, Springfield, Virginia 22161.

Contents

Contents (concluded)

List of Tables

List of Tables (concluded)

List of Figures

Executive Summary

Background and Site Information

There has been much concern over the potential hazards of landfill gas emissions. The predominant component of landfill gas emissions is methane, which is highly flammable and has been identified as a major greenhouse gas implicated in global warming. Another issue with landfill gas emissions is odor nuisance complaints due to trace constituents.

Recently research has begun on operating bioreactor landfills. The bioreactor process involves the injection of liquid such as leachate or sludge into the waste mass. In the case of aerobic bioreactor landfills, air is injected into the waste mass in addition to the liquid material to induce aerobic microorganisms to degrade the waste more rapidly. The goals of this technique are to increase landfill space (resulting in more cost-effective landfill practices), to bring the waste as close to full maturation as is feasible with the technology, and to eliminate both potential environmental threats from concentrated leachate and hazards associated with methane gas production.

The EPA and ARCADIS conducted a fugitive emission characterization study at the Three Rivers Solid Waste Technology Center Landfill located near Jackson, South Carolina. The survey area is a two-acre research and development site that practices leachate recirculation and air injection. The site is located in Cell 1 of the Three River Regional Subtitle D Landfill. The focus of this study was to evaluate emissions of fugitive gases, such as methane and hazardous air pollutants (HAPs) at the site.

Testing Procedures

Data was collected at the site using two open-path Fourier transform infrared (OP- FTIR) spectrometers and an open-path tunable diode laser absorption spectroscopy (OP- TDLAS) system. Three horizontal radial plume mapping (HRPM) surveys were done along the surface of the site to search for surface emissions hot spots. The last HRPM survey was conducted while leachate was being pumped (through a hose that extended diagonally across the surface of the survey area) from a small holding pond located in the southeast corner of the site to another small holding pond located in the northwest corner of the site. Vertical radial plume mapping (VRPM) surveys were performed over three days using two vertical configurations to measure emissions of fugitive gases and volatile organic compounds (VOCs) upwind and downwind of the top surface site.

Results and Discussion

HRPM Results

HRPM surveys conducted on 21 and 22 January 2004 detected the presence of a methane hot spot near the center of the site that had peak concentrations ranging from over 26 ppm to over 48 ppm above ambient background levels. An HRPM survey was conducted on the afternoon of 22 January with leachate being pumped from a small holding pond at the southeast corner of the site to another small holding pond located at the northwest corner of the site. This survey detected an additional methane hot spot located near the northwest corner of the site that had concentrations greater than 23 ppm above ambient background levels. This hot spot is probably associated with emissions from the leachate being pumped to the holding pond located at the northwest corner of the cell.

VRPM Results

VRPM surveys were done at the site on each day of the field campaign. Table E-1 presents the calculated methane fluxes from each survey.

Table ES-1. Average Calculated Methane Fluxes Found During the Upwind and Downwind VRPM Surveys.

Survey Date	Calculated Up-wind (Western) Methane Flux (g/s)	Calculated Down-wind (Eastern) Methane Flux (g/s)
1/20/2004	15	N/A[a]
1/21/2004	14[b]	10[c]
1/22/2004	20[b]	18[c]

[a] Downwind methane flux data from the 01/20/2004 VRM Survey is not available due to software problems in the field.
[b] Upwind methane flux data from 01/21 and 01/22/04 were collected with the OP-TDLAS instrument due to software problems with the Midac OP-FTIR.
[c] Calculated downwind methane flux values are lower than the corresponding upwind values because the entire methane plume was not captured by the downwind VRPM configuration.

The results of the VRPM surveys found that, in many cases, the upwind calculated methane fluxes were higher than the downwind methane fluxes. This was probably due to the fact that a methane hot spot may have been present on the side slope located on the western side of the survey area (directly upwind of the upwind VRPM configuration). Several relief wells were observed along the surface of this side slope, and elevated methane concentrations were measured along an OP-TDLAS beam path deployed in the vicinity of these wells. The existence of a methane hot spot along the side slope is also supported by the shape of the upwind methane plume maps generated by the VRPM software (see Section 3.2.1). The downwind methane flux values from 21 and 22 January are probably lower than the corresponding upwind values because the prevailing winds at the time of the surveys carried a large portion of the plume from the upwind hot spot outside of the downwind VRPM configuration, which was substantially shorter than the upwind VRPM configuration.

VOC and Ammonia Results

The datasets from the HRPM and VRPM surveys were searched for the presence of VOCs and ammonia. The analysis detected ammonia and methanol at the site. The measured ammonia concentrations ranged from 2.8 to 37 ppb. Methanol was detected only during the 21 January single-path measurements conducted with the leachate pump operating. The measured methanol concentration was 11 ppb.

Chapter 1
Project Description and Objectives

1.1 Background

There has been much concern over the potential hazards of landfill gas emissions. The predominant component of landfill gas emissions is methane, which is highly flammable and has been identified as a major greenhouse gas implicated in global warming. Another issue with landfill emissions is odor nuisance complaints due to trace constituents.

Recently, research has begun on operating bioreactor landfills. The bioreactor process involves the injection of liquid such as leachate or sludge into the waste mass. In the case of aerobic bioreactor landfills, air is injected into the waste mass in addition to the liquid to induce aerobic microorganisms to degrade the waste more rapidly. The goals of this technique are to increase landfill space (resulting in more cost-effective landfill practices), to bring the waste as close to full maturation as is feasible with the technology, and to eliminate potential environmental threats due to concentrated leachate and hazards associated with methane gas production.

EPA and ARCADIS conducted a fugitive emission characterization study at the Three Rivers Solid Waste Technology Center Landfill located near Jackson, SC. The survey site is a two- acre research and development area located in Cell 1 of the Three River Regional Subtitle D Landfill (see Figure 1-1).

The landfill system includes a network of piping that collects and injects leachate from the Three Rivers Regional Landfill into the waste while, at the same time, injecting air into the waste in order to stimulate aerobic conditions within the landfill to initiate and maintain the rapid decay of waste. The survey area is approximately 60 feet deep and consists of about 70,000 cubic yards of waste and daily cover.

Figure 1-1. Survey Area at the Three Rivers Landfill.

The focus of this study is to evaluate emissions of fugitive gases such as methane and hazardous air pollutants (HAPs) at the site using an open-path Fourier transform infrared (OP-FTIR) spectrometer and an open-path tunable diode laser absorption spectroscopy (OP-TDLAS). The study involved a technique developed through research funded by the U.S. Environmental Protection Agency (EPA) National Risk Management Research Laboratory (NRMRL), which uses ground-based optical remote sensing instrumentation, known as radial plume mapping (RPM) (Hashmonay and Yost, 1999;

Hashmonay et al., 1999; Wu et al., 1999; Hashmonay et al., 2001; Hashmonay et al., 2002). The survey identified emission hot spots (areas of relatively higher emissions), investigated source homogeneity, and calculated an emission flux rate for methane detected at the site. Concentration maps in the horizontal and downwind vertical planes were generated using the horizontal radial plume mapping (HRPM), and vertical radial plume mapping (VRPM) methods, respectively.

The study consisted of one field campaign performed during January 2004 by EPA and ARCADIS personnel.

1.2 Project Description and Purpose

The optical remote scanning (ORS) techniques used in this study were designed to characterize the emissions of fugitive gases from area sources. Spatial information is obtained from multi-path ORS measurements by the use of iterative search algorithms. The HRPM method involves the use of a configuration of nonoverlapping radial beam geometry to map the concentration distributions in a horizontal plane. The VRPM method is applied to a vertical plane downwind from an area emission source to map the crosswind and vertical profiles of a plume. By incorporating wind information, the flux through the plane is calculated, which leads to an emission rate of the upwind area source. An OP-FTIR sensor was chosen as the primary instrument for the study because of its capability of accurately measuring a large number of chemical species that might occur in a plume.

The OP-FTIR spectrometer combined with the RPM method is designed for both fence-line monitoring applications, and real-time, on-site, remediation monitoring and source characterization. An infrared light beam modulated by a Michelson interferometer is transmitted from a single telescope to a retro-reflector (mirror) target, which is usually set up at a range of 100 to 500 meters. The returned light signal is received by the single telescope and directed to a detector. Some of the light is absorbed by the molecules in the beam path as the light propagates to the mirror, and more is absorbed as the light is reflected back to the analyzer. Thus, the round-trip path of the light doubles the chemical absorption signal. One advantage of OP-FTIR monitoring is that the concentrations of a multitude of infrared absorbing gaseous chemicals can be detected and measured simultaneously with high temporal resolution.

The OP-TDLAS system (Unisearch Associates) is a fast, interference-free technique for making continuous concentration measurements of many gases. The OP-TDLAS used in the current study is capable of measuring concentrations over an open path up to 1 km in the range of tens of parts per billion for gases such as carbon monoxide (CO), carbon dioxide (CO_2), ammonia (NH_3), and methane (CH_4). The laser emits radiation at a particular wavelength when an electrical current is passed through it. The light wavelength depends on the current and, therefore, allows scanning over an absorption feature and analyzing for the target gas concentration using Beer's law. The OP-TDLAS used in this study is a multiple channel TDL instrument that allows fast scanning electronically (few seconds) among many beam-paths (presently, 8 beams). The OP-TDLAS applies a small 4-inch telescope, which launches the laser beam to a mirror. The laser beam is returned by the mirror to the telescope, which is connected with fiber optics to a control box that houses the laser and a multiple channel detection device. For this particular field campaign, data from the OP-TDLAS were used to provide information on methane concentrations at the site. Figure 1-2 shows a picture of the OP-TDLAS system used in the current study.

Meteorological and survey measurements were also made during the field campaign. A theodolite was used to make the survey measurement of the azimuth and elevation angles and the radial distances to the mirrors, relative to the OP-FTIR sensor.

The objectives of the study are:

- Collect OP-FTIR data in order to identify major emissions hot spots by generating surface concentration maps in the horizontal plane, and

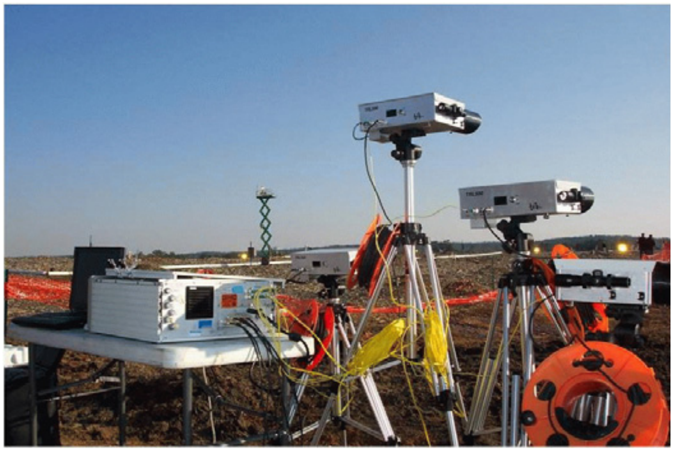

Figure 1-2. OP-TDLAS System.

- Measure emission fluxes of detectable compounds downwind from major hot spots.

1.2.1 Horizontal RPM

The HRPM approach provides spatial information to path-integrated measurements acquired in a horizontal plane by an ORS system. This technique yields information on the two-dimensional distribution of the concentrations in the form of chemical concentration contour maps. This form of output readily identifies chemical "hot spots," the location of high emissions. This method can be of great benefit for performing site surveys before, during, and after site remediation activities.

HRPM scanning is usually performed with the ORS beams located as close to the ground as is practical. This enhances the ability to detect minor constituents emitted from the ground since the emitted plumes dilute significantly at higher elevations. The survey area is typically divided into a Cartesian grid of n times m rectangular cells. In some unique cases, the survey area may not be rectangular due to obstructions, and the shape of the cells may be slightly altered accordingly. A mirror is located in each of these cells, and the ORS sensor scans to each of these mirrors, dwelling on each for a set measurement time (30 seconds in the present study). The system scans to the mirrors in the order of either increasing or decreasing azimuth angle. The path-integrated concentrations measured at each mirror are averaged over several scanning cycles to produce concentration maps that are time-averaged (Hashmonay et al., 1999). Meteorological measurements are made concurrent to the scanning measurements.

Figure 1-3 represents a typical HRPM configuration. In this particular case, $n = m = 3$. The solid lines represent the nine optical paths, each terminating at a mirror.

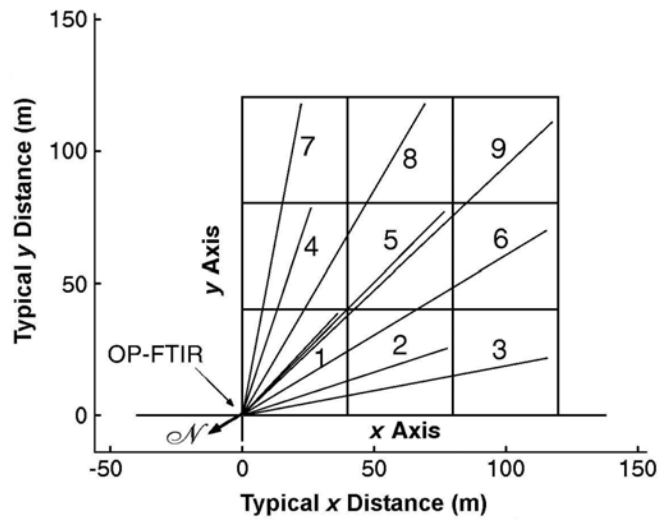

Figure 1-3. Example of a HRPM Configuration.

One OP-FTIR instrument (manufactured by IMACC, Inc.) was used to collect horizontal RPM data during the field campaign.

1.2.2 Vertical RPM

The VRPM method maps the concentrations in the vertical plane by scanning the ORS system in a vertical plane downwind from an area source. The plane-integrated concentration can be obtained from the reconstructed concentration maps. The flux is calculated by multiplying the plane-integrated concentration by the wind speed component perpendicular to the vertical plane. Thus, the VRPM method leads to a direct measurement-based determination of the upwind source emission rate (Hashmonay et al., 1998; Hashmonay and Yost, 1999, Hashmonay et al., 2001).

Figure 1-4 shows a schematic of the experimental setup used for vertical scanning. Several mirrors are placed in various locations on a vertical plane in-line with the scanning OP FTIR. A vertical platform (scissors jack) is used to place two of the mirrors at a predetermined height above the surface. The location of the vertical plane is selected so that it intersects the mean wind direction as close to perpendicular as practical. Two OP-FTIR instruments (manufactured by Midac, Inc. and IMACC, Inc.) were used to complete the VRPM surveys.

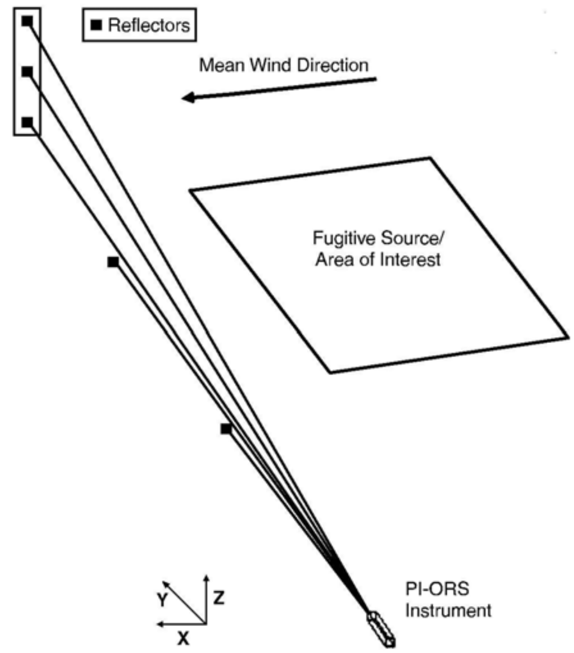

Figure 1-4. Example of a VRPM Configuration.

1.3 Quality Objectives and Criteria

Data quality objectives (DQOs) are qualitative and quantitative statements developed using EPA's DQO process (U.S. EPA, 2000) that clarify study objectives, define the appropriate type of data, and specify tolerable levels of potential decision errors that will be used as the basis for establishing the quality and quantity of data needed to support decisions. DQOs define the performance criteria that limit the probabilities of making decision errors by considering the purpose of collecting the data, defining the appropriate type of data needed, and specifying tolerable probabilities of making decision errors.

Quantitative objectives are established for critical measurements using the data quality indicators (DQIs) of accuracy, precision, and completeness. The acceptance criteria for these DQIs are summarized in Table 1-1. Accuracy of measurement parameters is determined by comparing a measured value to a known standard, assessed in terms of percent bias. Values must be within the listed tolerance to be considered acceptable.

Table 1-1. DQI Goals for Critical Measurements.

Parameter	Analysis Method	Accuracy (% bias)	Precision (%RSD)	Completeness
Analyte PIC[a]	OP-FTIR: nitrous oxide concentrations	±25%/15%/10%[b]	±10%	90%
Ambient Wind Speed	Climatronics Met heads side-by-side comparison in the field	±1 m/s	±1 m/s	90%
Ambient Wind Direction	Climatronics Met heads side-by-side comparison in the field	±10°	±10°	90%
Distance	Theodolite- Topcon	±1 m	±1 m	100%

[a] PIC = path-integrated concentration.
[b] The accuracy acceptance criterion of ±25% is for pathlengths of less than 50m, ±15% is for pathlengths between 50 and 100m, and ±10% is for pathlengths greater than 100m.

Precision is evaluated by making replicate measurements of the same parameter and by assessing the variations of the results. Precision is assessed in terms of relative percent difference (RPD), or relative standard deviation (RSD). Replicate measurements are expected to fall within the tolerances shown in Table 1-1. Completeness is expressed as a percentage of the number of valid measurements compared to the total number of measurements taken.

Estimated minimum detection limits (MDLs) of the OP-FTIR instrument are given by compound in Table 1-2. It is important to note that the values listed in Table 1-2 should be considered first step approximations because the MDL is highly variable and depends on many factors including atmospheric conditions. Actual MDLs are calculated in the quantification software for all measurements taken. Minimum detection levels for each absorbance spectrum are determined by calculating the root mean square (RMS) absorbance noise in the spectral region of the target absorption feature. The MDL is the target compound absorbance signal that is five times the RMS noise level, using a reference spectrum acquired for a known concentration of the target compound. Guidance documents such as Compendium Method TO-16 (U.S. EPA, 1999) and American Society for Testing and Materials (ASTM) Standard Practices E1982-98 (ASTM, 1999) typically define estimated minimum detection limits (MDL) as 3 times the RMS noise. However, signals at this level may be due to the presence of a given compound or may be false positives. The estimate of five times the RMS noise reduces the probability of measuring false positives and was therefore used in the analysis of the current data set to provide more conservative results.

Table 1-2. Detection Limits for Target Compounds.

Compound	OP-FTIR Estimated Detection Limit for Path Length = 100m, 1 min Average (ppmv)	AP-42 Value as a ratio to an average methane concentration of 50 ppm[a] (ppmv)
1,4-Dichlorobenzene	0.012	0.000021
2-Propanol	0.0060	0.0050
Acetone	0.024	0.00070
Acrylonitrile	0.010	0.00063
Ammonia	0.0040	N/A[b]
Butane	0.0060	0.00050
Chlorobenzene	0.040	0.000025
Chloroform	0.012	0.0000030
Chloromethane	0.012	0.00010
Dichlorodifluoromethane	0.0040	0.0016
Dimethyl sulfide	0.018	0.00078
Ethane	0.010	0.089
Ethanol	0.0060	0.0027
Ethyl benzene	0.060	0.00046
Ethyl chloride	0.0040	0.00013
Ethylene dibromide	0.0060	0.00000010

continued

Table 1-2. Detection Limits for Target Compounds (concluded).

Compound	OP-FTIR Estimated Detection Limit for Path Length = 100m, 1 min Average (ppmv)	AP-42 Value as a ratio to an average methane concentration of 50 ppm[a] (ppmv)
Ethylene dichloride	0.030	0.000041
Fluorotrichloromethane	0.0040	0.000076
Hexane	0.0060	0.00066
Hydrogen sulfide	6.0	0.0036
Methane	0.024	N/A
Methanol	0.0015	N/A
Methyl ethyl ketone	0.030	0.00071
Methyl isobutyl ketone	0.040	0.00019
Methyl mercaptan	0.060	0.00025
Methylene chloride	0.014	0.0014
Octane	0.0025	N/A
Pentane	0.0080	0.00033
Propane	0.0080	0.0011
Propylene dichloride	0.014	0.000018
Tetrachloroethene	0.0040	0.00037
Trichlorethylene	0.0040	0.00028
Vinyl chloride	0.010	0.00073
Vinylidene chloride	0.014	0.000020
Xylenes	0.030	0.0012

[a] The AP-42 values represent an average concentration of different pollutants in the raw landfill gas. This is not comparable to the detection limits for the OP-FTIR which is an average value for a path length of 100 meters across the surface of the area source being evaluated. However, it does provide an indication of the types of pollutants and range of concentrations associated with landfill gas emissions in comparison to the detection limits of the OP-FTIR.

[b] N/A = not available.

1.4 Project Schedule

The field campaign for this study was completed during January 2004. Table 1-3 provides the schedule of ORS work that was performed.

Table 1-3. Schedule of Work Performed at the Site.

Day (2004)	Detail of Work Performed	Notes
Tuesday, 20 January 2004	PM-VRPM survey of site	Due to software problems, downwind VRPM data was not available from this survey
Wednesday, 21 January 2004	AM-VRPM survey of site PM-HRPM survey of site PM-VRPM survey of site	Data from AM VRPM survey was not reported because the wind data failed to meet the acceptance criteria
Thursday, 22 January 2004	AM-HRPM survey of site PM-VRPM survey of site PM-HRPM survey of site while leachate pump was operating	

Chapter 2
Testing Procedures

The following subsections describe the testing procedures used at the site. HRPM was performed along the surface of the survey area to produce surface concentration maps and to locate any emissions hot spots. VRPM was performed using two OP-FTIR instruments, and the OP-TDLAS system. The coordinates of the mirrors used in each configuration (relative to the position of the ORS instrument) are presented in Appendix A and B.

OP-FTIR raw data were collected as interferograms. All data were archived to CD-ROMs. After archiving, interferograms were transferred to ARCADIS. They were then transformed to single beam spectra, and concentrations were calculated using Non-Lin (Spectrosoft) quantification software. This analysis was done after completion of the field campaign. Concentration data were then matched with the appropriate mirror locations, wind speed, and wind direction. The ARCADIS RPM software was used to process the data into horizontal plane or vertical plane plume visualizations, as appropriate.

Meteorological data including wind direction, wind speed, temperature, relative humidity, and barometric pressure were continuously collected during the measurement campaign with an automated R.M. Young instrument. It collected real-time data from its sensors and recorded time-stamped data as one-second averages to the data collection computer. Sensing heads for wind direction and speed were used to collect data at the surface during the HRPM surveys and at 2 and 10 meters heights during the VRPM survey (the 10-m sensor was placed on top of the scissors jack that held the mirrors). The sensing heads for wind direction incorporate an auto-north function (automatically adjusts to magnetic north) that eliminates the errors associated with subjective field alignment to a compass heading. After data collection, a linear interpolation between the two sets of data was done to estimate wind velocity as a function of height.

Once the concentrations maps and wind information were processed, the concentration values were integrated, incorporating the wind speed component normal to the plane at each height level to compute the flux through the vertical plane. In this stage, the concentration values were integrated from parts per million by volume to grams per cubic meter, considering the molecular weight of the target gas. This enables the direct calculation of the flux in grams per second, using wind speed data in meters per second.

The concordance correlation factor (CCF) is used to represent the level of fit for the reconstruction in the path-integrated domain—predicted vs. observed path-integrated concentration (PIC). The CCF is similar to the Pearson correlation coefficient (r), but is adjusted to account for shifts in location and scale. Like the Pearson correlation, CCF values are bounded between -1 and +1, yet the CCF can never exceed the absolute value of the Pearson correlation factor. For example, the CCF will be equal to the Pearson correlation when the linear regression line intercepts the ordinate at 0, and its slope equals 1. Its absolute value will be lower than the Pearson correlation when the above conditions are not met. For the purposes of this report, the closer the CCF value is to +1, the better the fit for the reconstruction in the path-integrated domain.

In reporting the average calculated flux, a moving average is used in the calculation of the average flux values to show temporal variability in the measurements. A moving average involves averaging flux values calculated from several different consecutive cycles (a cycle is defined as data collected when scanning one time through all the mirrors in the configuration). For example, a data set taken from 5 cycles may be reported using a moving average of 4, where values from cycles 1 to 4, and 2 to 5 are averaged together to show any variability in the flux values.

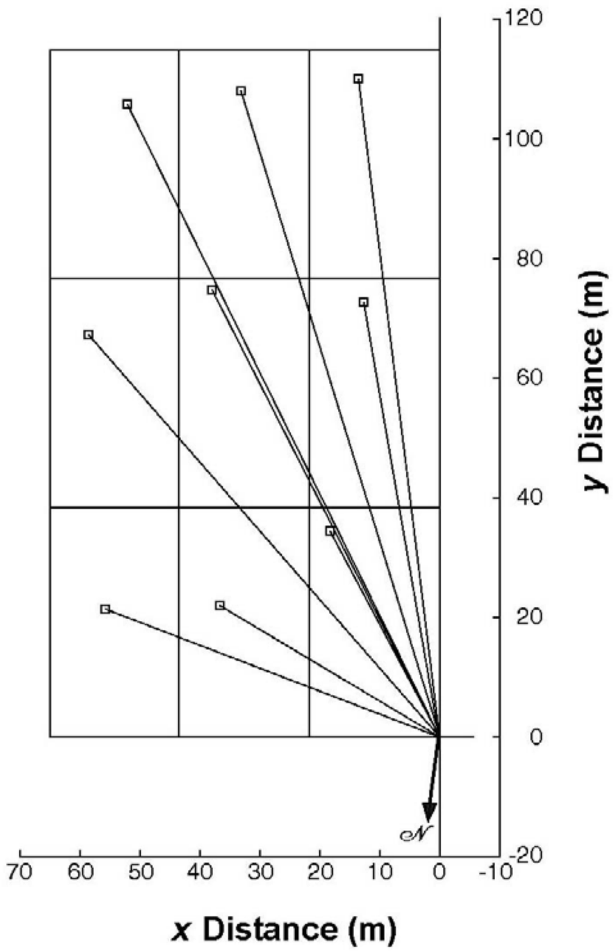

Figure 2-1. Schematic of the HRPM Configuration Used During the 01/21/04 Survey.

2.1 HRPM Surveys

One HRPM survey was conducted along the surface of the survey area on 21 January 2004 and two HRPM surveys were conducted on 22 January 2004. During the second HRPM survey on 22 January, leachate was being pumped (through a hose that extended diagonally across the surface of the survey area from a small holding pond at the southeast corner of the site to another small holding pond at the northwest corner of the site. During the HRPM surveys, the optical paths were configured as close to the surface of the cell as possible (less than one meter above the surface). Figures 2-1 and 2-2 present the HRPM configurations used during the 21 and 22 January HRPM surveys, respectively. The solid lines represent the nine optical paths used in the configuration, each terminating at a mirror. The same terrain

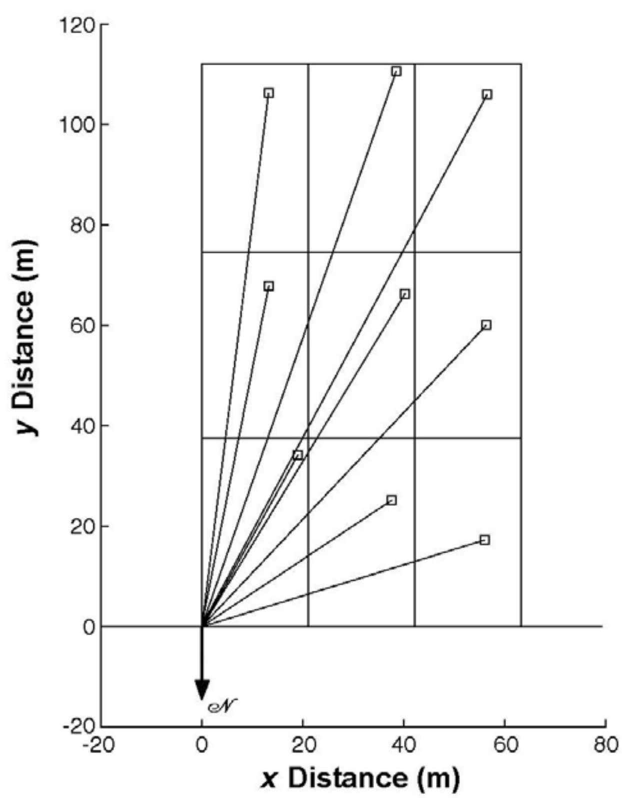

Figure 2-2. Schematic of the HRPM Configuration Used During the 01/22/04 Surveys.

was surveyed on both days, but the OP-FTIR was placed in a different corner of the area on each day.

2.2 VRPM Measurements

VRPM surveys were conducted at the site during each day of the field campaign using two ORS instruments. The VRPM surveys were completed using two vertical configurations set up along the eastern and western boundary of the survey area. Due to geographical limitations at the site, the VRPM configuration along the eastern boundary of the site was limited to a distance of 95 meters. Figure 2-3 presents the overall layout of the site and the location of the VRPM configurations used during 20 January. Figure 2-4 shows the location of the VRPM configurations used during 21 and 22 January. In both figures, the blue cylinders indicate the locations of the ORS instruments, and the blue squares indicate the locations of the scissors jacks (vertical structures) used in the configurations.

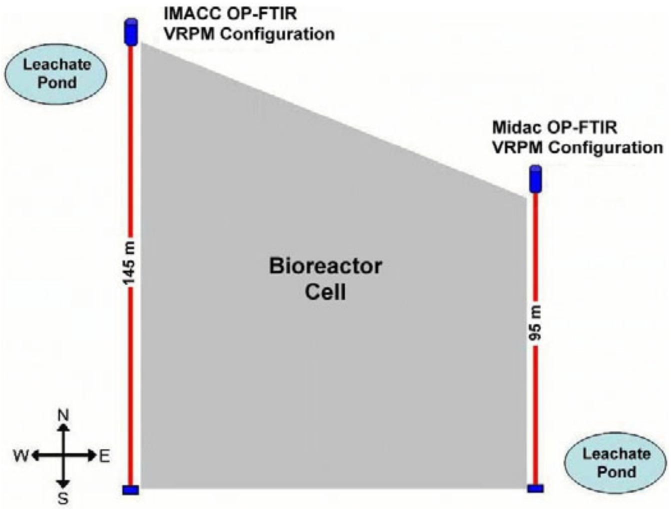

Figure 2-3. Map of Three Rivers Landfill Showing the Location of the Survey Site and the VRPM Configurations Used During 01/20/04 Survey.

During each survey, one vertical configuration served as the upwind measurement of the top surface of the site, and the other served as the downwind measurement of the top surface, depending on the prevailing wind direction. The use of an upwind VRPM configuration allowed for the identification of any upwind source and the calculation of a flux value for the identified sources.

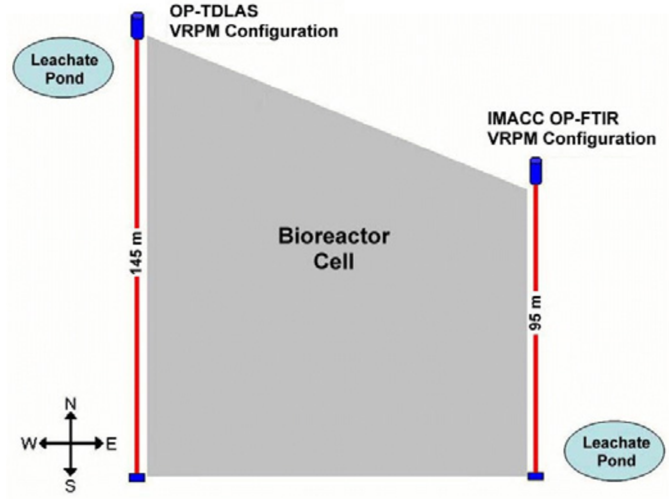

Figure 2-4. Map of Three Rivers Landfill Showing the Location of the Survey Site and the VRPM Configurations Used During 01/21 and 01/22/04 Surveys.

2.2.1 VRPM Survey of 20 January 2004

The observed wind direction was westerly during the VRPM survey of 20 January. The IMACC instrument was located along the western boundary (upwind) of the survey area, and the Midac instrument was located along the eastern boundary (downwind) of the area. The upwind configuration consisted of three mirrors placed along the surface and two mirrors placed on the upwind scissors jack. Due to software problems with the scanner controlling the Midac instrument, data was not collected with this instrument.

2.2.2 VRPM Surveys of 21 January 2004

Two VRPM surveys were conducted at the site on 21 January. During the morning VRPM survey, the observed wind direction was southeasterly, and the Midac OP-FTIR was located along the eastern boundary (upwind) of the survey area and the IMACC OP-FTIR along the western boundary (downwind). Each configuration consisted of three mirrors placed along the surface and two mirrors placed on the scissors jack. Figure 2-5 shows a picture of the upwind configuration used during the survey.

Figure 2-5. Upwind Configuration from the Morning VRPM Survey on 01/21/04.

During the afternoon VRPM survey, the observed wind direction was southwesterly. Due to software problems with the Midac OP-FTIR scanner, the IMACC OP-FTIR was set up along the eastern boundary to ensure that downwind data was collected. The OP-TDLAS system was set up along the cell's western boundary to collect upwind methane concentration data. The upwind and downwind configurations consisted of three mirrors placed along the surface, and two mirrors placed on the scissors jack.

2.2.3 VRPM Survey of 22 January 2004

During the VRPM survey of 22 January, the observed wind direction was westerly. Due to continued technical problems with the Midac OP-FTIR scanner, the IMACC OP-FTIR was set up along the eastern boundary to ensure that downwind data was collected. The OP-TDLAS system was set up along the western boundary of the cell to collect upwind methane concentration data. The upwind and downwind configurations consisted of three mirrors placed along the surface, and two mirrors placed on the scissors jack.

2.3 Single Path Measurement during Leachate Pump Operation

During the afternoon of 21 January, leachate was being pumped from a holding pond adjacent to the site through a hose that extended diagonally across the surface of the survey area. At the request of the site operator, data was collected with the OP-FTIR to measure any emissions coming from the hose. For this survey, one mirror was placed directly beyond the leachate hose at a distance of 86.4 meters from the OP-FTIR instrument.

2.4 OP-TDLAS Measurements

The OP-TDLAS system was deployed for each day of the field campaign along the western boundary of the survey area. The OP-TDLAS configuration was similar to the configuration used on the western side of the cell during the VRPM surveys of 20 January, and the morning of 21 January. As mentioned previously, the OP-TDLAS system was used to provide upwind data for the VRPM surveys on 21 and 22 January due to technical problems with one of the OP-FTIR instruments. Figure 2-6 shows a picture of the OP-TDLAS configuration used at the site.

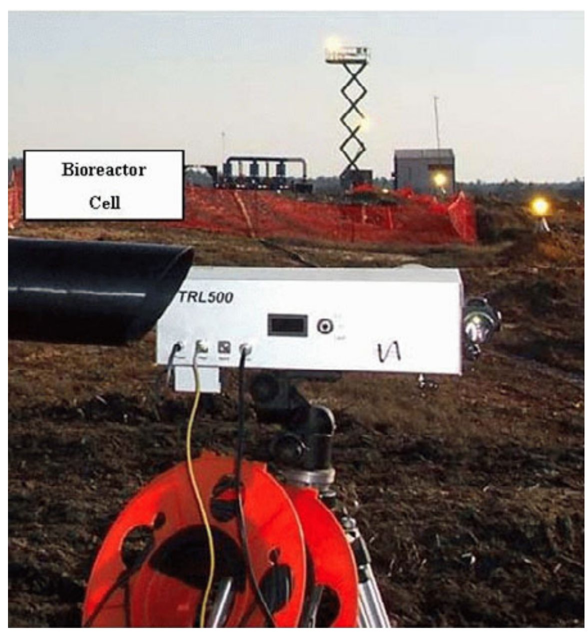

Figure 2-6. OP-TDLAS Configuration Used at the Site.

Chapter 3
Results and Discussion

The results from the ORS data collected at the site are presented in the following subsections. The measured methane concentrations from the HRPM and VRPM surveys are presented in Appendix C.

3.1 The Horizontal RPM Results

HRPM surveys were conducted at the site to detect methane hot spots. Figure 3-1 presents the reconstructed map of average surface methane concentrations (in parts per million—ppm) found during the HRPM survey of 21 January. The contours give methane concentration values (in parts per million) above ambient background concentrations. The red dot indicates the location of the OP-FTIR and scanner. The figure shows the presence of a hot spot near the center of the site (concentrations greater than 48 ppm above ambient background).

Figure 3-2 presents the reconstructed map of average surface methane concentrations (in parts per million) found during the HRPM survey done on the morning of 22 January. The figure shows the presence of a hot spot near the center of the site (concentrations greater than 36 ppm above ambient background). The location of the methane hot spot found during this survey is very similar to the results found during the HRPM survey of 21 January.

Figure 3-3 presents the reconstructed map of average surface methane concentrations (in parts per million) found during the HRPM survey done on the afternoon of 22 January. During this survey, leachate was being pumped, as described earlier in Section 2.1.

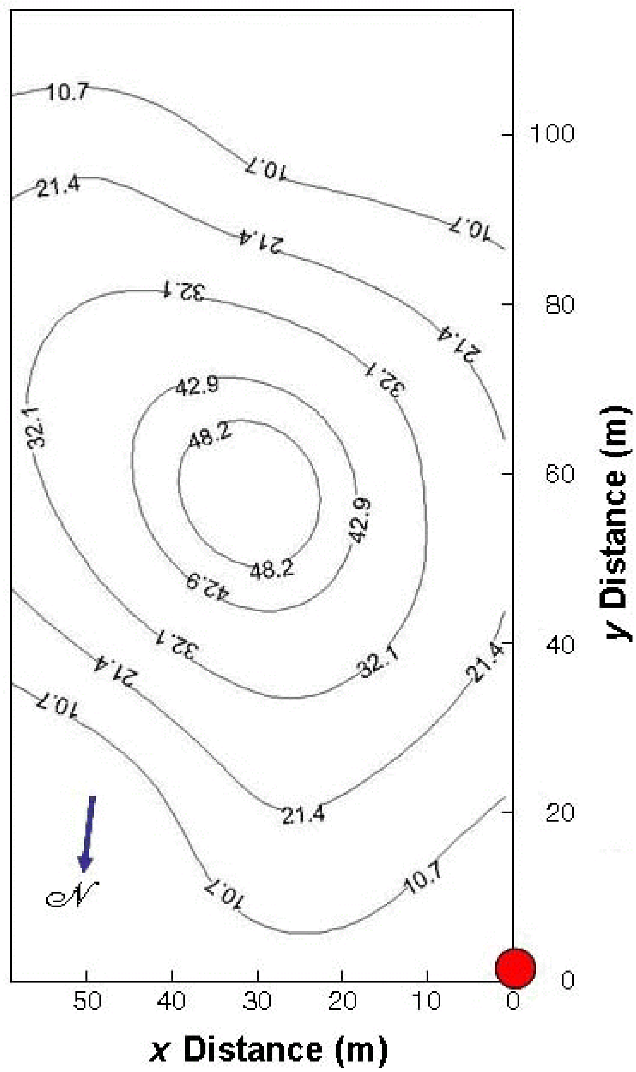

Figure 3-1. Average Surface Methane Concentration Contour Map from the HRPM Survey of 01/21/04 .

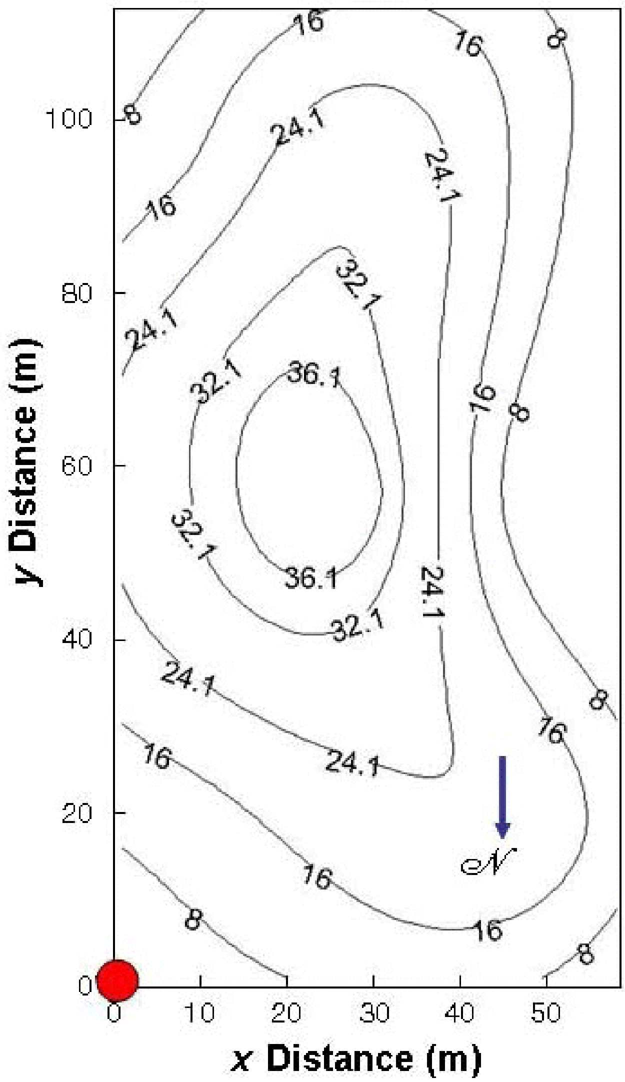

Figure 3-2. Average Surface Methane Concentration Contour Map from 01/22/04 Morning HRPM Survey.

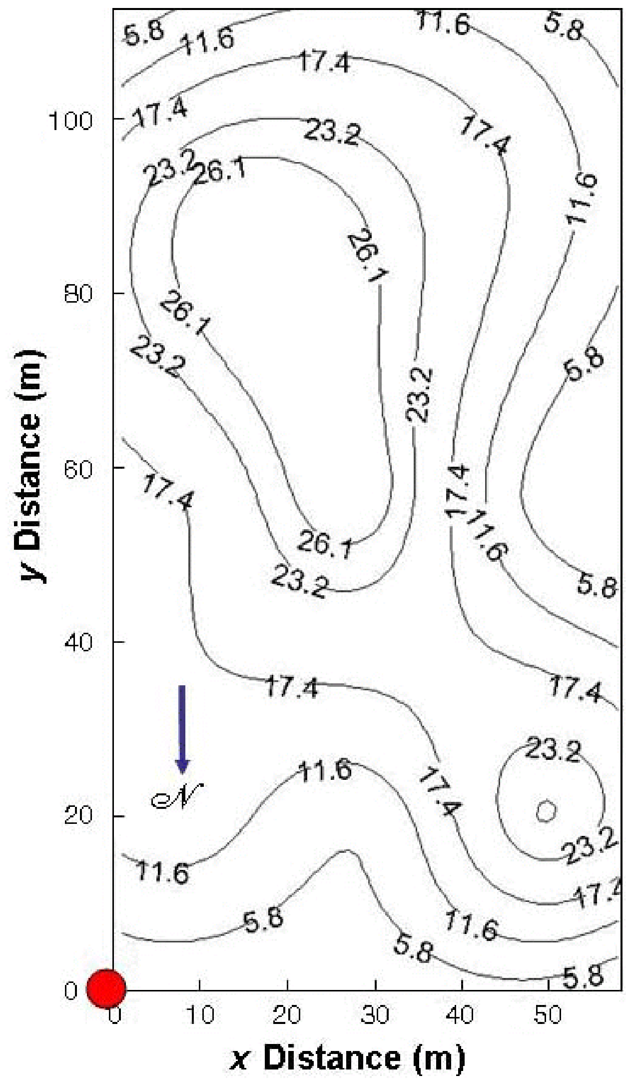

Figure 3-3. Average Surface Methane Concentration Contour Map from 01/22/04 Afternoon HRPM Survey.

The figure shows the presence of a hot spot near the center of the site (concentrations greater than 26 ppm above ambient background), and a hot spot near the northwest corner (concentrations greater than 23 ppm above ambient background). The hot spot in the northwest portion of the site (which was not present during the previous HRPM surveys) is probably due to emissions from the leachate being pumped to the holding pond located in the northwest corner of the cell.

3.2 The Vertical RPM Results

As mentioned previously, the VRPM surveys were completed using two vertical configurations set up along the eastern and western boundary of the survey area. During each survey, one vertical configuration served as the upwind measurement of the top surface of the area, and the other served as the downwind measurement of the top surface, depending on the prevailing wind direction.

3.2.1 VRPM Survey of 20 January 2004

During the 20 January VRPM survey, the observed wind direction was west-northwest. The upwind configuration was located along the western boundary of the area, and the downwind configuration was located along the eastern boundary. Due to software problems with the Midac OP-FTIR system located along the eastern boundary of the area, downwind data was not available for this particular survey. Table 3-1 presents the calculated methane fluxes measured along the upwind VRPM plane.

Table 3-1. Moving Average of Calculated Methane Flux, CCF, Wind Speed, and Wind Direction for 01/20/04 Upwind VRPM Survey.

Cycles	CCF	Flux (g/s)	Wind Speed (m/s)	Relative Wind Dir.[a] (deg)	Absolute Wind Dir. (deg from North)
1 to 3	0.908	11	1.7	35	305
2 to 4	0.960	10	1.6	43	313
3 to 5	0.934	13	1.8	35	305
4 to 6	0.855	17	1.8	22	292
5 to 7	0.907	17	1.9	13	283
6 to 8	0.916	13	1.5	1	271
7 to 9	0.983	14	1.5	7	277
8 to 10	0.918	18	1.4	17	287
9 to 11	0.802	20	1.5	33	303
10 to 12	0.888	15	1.3	29	299
Std. Dev.		**3.25**			

[a] Relative wind direction shown is the angle from a vector normal to the plane of the configuration.

Figure 3-4 presents the reconstructed methane plume from the upwind VRPM plane. Contour lines give methane concentrations (in parts per million) above ambient background concentration. The average calculated methane flux from the upwind plane was 15 g/s. The shape of the plume shown in Figure 3-4 is not very broad vertically, and the concentrations found along the surface are not homogenous. This suggests that a methane hot spot may have been located in an upwind location close to the VRPM plane.

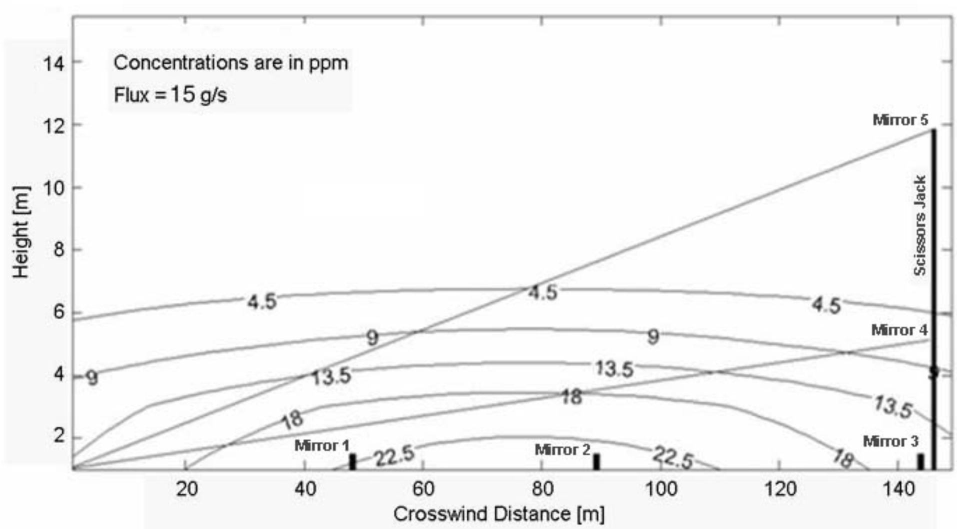

Figure 3-4. Average Reconstructed Methane Plume from the 01/20/04 Upwind VRPM Survey.

3.2.2 VRPM Surveys of 21 January 2004

Two VRPM surveys were conducted at the site on 21 January. During the morning VRPM survey, the observed winds were from the south-southeast. The necessary wind criteria to obtain valid flux measurements is that the observed wind direction must be ± 70º from perpendicular to the angle of the vertical planes used in the measurements. A closer analysis of the wind data collected during the morning VRPM run revealed that during most of the data collection period, the winds failed to meet this criteria. Consequently, the data from the morning VRPM survey will not be reported.

During the afternoon VRPM survey, the observed winds were from the southwest. Due to continuing software problems with the Midac OP-FTIR instrument, the IMACC OP-FTIR was set up along the eastern boundary of the site to ensure that downwind data was collected. The OP-TDLAS system was set up along the western boundary of the cell to collect upwind methane concentration data. A study was conducted during the current field campaign to compare methane concentrations measured with the OP-FTIR and OP-TDLAS instruments along the same path length. The results found favorable agreement between the two instruments. More information on this study can be found in Section 5.6 of this report.

Tables 3-2 and 3-3 present the calculated methane fluxes measured along the upwind and downwind vertical planes during the afternoon VRPM survey, respectively.

Table 3-2. Moving Average of Calculated Methane Flux, CCF, Wind Speed, and Wind Direction for 01/21/04 Afternoon Upwind VRPM Survey (Collected with OP-TDLAS)

Cycles	CCF	Flux (g/s)	Wind Speed (m/s)	Relative Wind Dir.[a] (deg)	Absolute Wind Dir. (deg from North)
1 to 3	0.955	18	2.9	311	221
2 to 4	0.960	15	2.5	307	217
3 to 5	0.975	13	2.5	313	223
4 to 6	0.996	11	2.5	305	215
5 to 7	0.985	15	2.2	336	246
6 to 8	0.944	15	1.6	359	269
7 to 9	0.936	15	1.7	354	264
8 to 10	0.967	13	1.8	328	238
9 to 11	0.990	9.7	2.3	302	212
10 to 12	0.997	8.7	2.1	309	219
Std. Dev.		**2.65**			

[a] Relative wind direction shown is the angle from a vector normal to the plane of the configuration.

Table 3-3. Moving Average of Calculated Methane Flux, CCF, Wind Speed, and Wind Direction for 01/21/04 Afternoon Downwind VRPM Survey (Collected with OP-FTIR)

Cycles	CCF	Flux (g/s)	Wind Speed (m/s)	Relative Wind Dir.[a] (deg)	Absolute Wind Dir. (deg from North)
1 to 3	0.813	9.9	2.9	317	222
2 to 4	0.616	18	2.5	313	218
3 to 5	0.639	21	2.5	322	227
4 to 6	0.940	16	2.5	312	217
5 to 7	0.981	13	2.2	337	242
6 to 8	0.988	11	1.6	359	264
7 to 9	0.990	10	1.8	354	259
8 to 10	0.980	6.7	1.8	330	235
9 to 11	0.911	4.5	2.3	306	211
10 to 12	0.998	7.5	2.1	313	218
Std. Dev.		**5.16**			

[a] Relative wind direction shown is the angle from a vector normal to the plane of the configuration.

Figures 3-5 and 3-6 present the reconstructed methane plume from the upwind and downwind 21 January afternoon VRPM surveys, respectively. Contour lines give methane concentrations (in parts per million) above ambient background concentration. The average calculated methane flux was 14 g/s for the upwind survey and 10 g/s for the downwind survey.

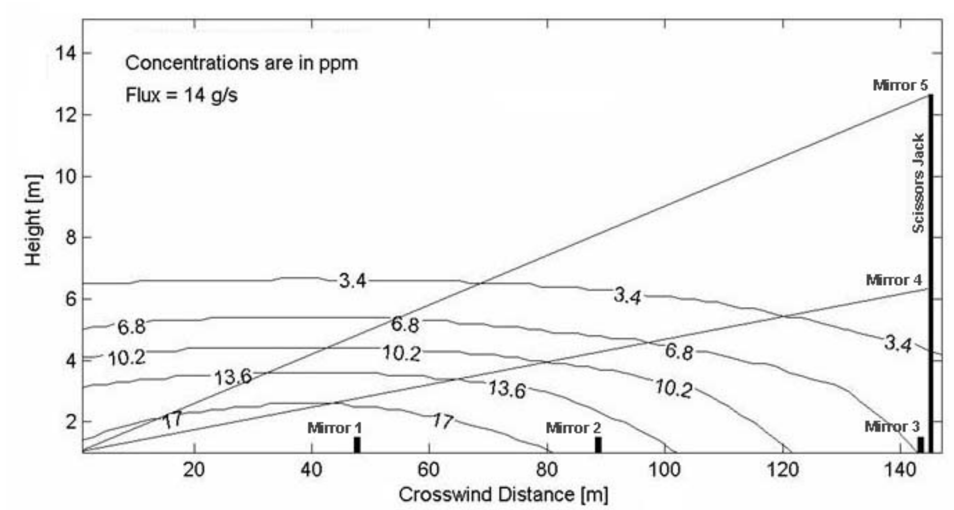

Figure 3-5. Average Reconstructed Methane Plume from the 01/21/04 Afternoon Upwind VRPM Survey.

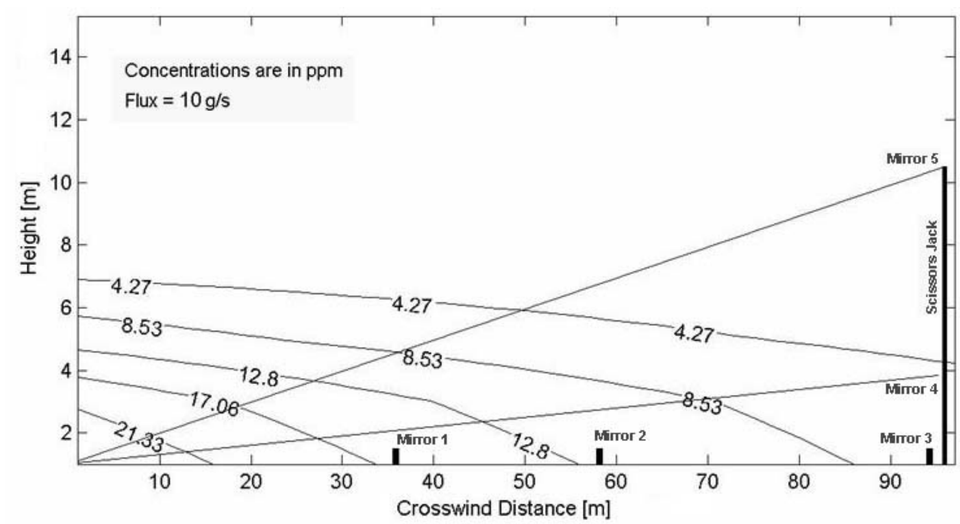

Figure 3-6. Average Reconstructed Methane Plume from the 01/21/04 Afternoon Downwind VRPM Survey.

The shape of the plume from the upwind VRPM survey shown in Figure 3-5 is not well developed vertically and not homogeneous in the horizontal direction, suggesting that a methane hot spot may have been located upwind, close to the upwind VRPM plane. This conclusion is supported by the fact that several relief wells were observed along the surface of the slope adjacent to the western boundary of the site, and elevated methane concentrations were measured along an OP-TDLAS beam path deployed in the vicinity of these wells.

The average methane flux during the upwind VRPM survey (14 g/s) was higher than the average flux measured during the downwind VRPM survey (10 g/s). It should be noted that these flux values are average values from all of the data collected during the survey. Tables 3-2 and 3-3 present a moving average of the calculated methane flux from the upwind and downwind configurations, respectively. The maximum calculated methane flux value from the upwind VRPM survey was 18 g/s, while at the same time, the maximum calculated methane flux value from the downwind VRPM survey was 21 g/s. It is apparent that, under certain wind conditions, the downwind VRPM survey calculated higher methane flux values than the upwind VRPM survey.

The flux measurements from the upwind VRPM survey were probably influenced primarily by emissions from the area of elevated methane located directly upwind of the site. The prevailing southwesterly winds observed during the survey may have carried most of the emissions from the upwind methane hot spot through the upwind VRPM configuration (base path length of 145 m). However, the prevailing winds probably caused most of the emissions from this hot spot to be carried outside of the much shorter downwind VRPM configuration (base path length of 95 m). Therefore, the flux measurements from the downwind VRPM survey may have been only slightly influenced by emissions from the hot spot upwind of the site. The flux measured from the downwind survey is probably due to emissions from the methane hot spot found near the center of the site during the HRPM survey (see Figure 3-1).

3.2.3 VRPM Survey of 22 January 2004

During the 22 January VRPM survey, the observed wind direction was from the west-northwest. The OP-TDLAS system (upwind) was located along the western boundary of the site, and the IMACC OP-FTIR (downwind) was located along the eastern boundary of the cell. Tables 3-4 and 3-5 present the calculated methane fluxes measured along the upwind and downwind vertical planes, respectively.

Table 3-4. Moving Average of Calculated Methane Flux, CCF, Wind Speed, and Wind Direction for 01/22/04 Upwind VRPM Survey (Collected with OP-TDLAS)

Cycles	CCF	Flux (g/s)	Wind Speed (m/s)	Relative Wind Dir.[a] (deg)	Absolute Wind Dir. (deg from North)
1 to 3	0.966	19	4.4	16	286
2 to 4	0.965	20	4.5	19	289
5 to 7	0.973	21	4.2	9	279
6 to 8	0.973	21	4.1	14	284
7 to 9	0.976	21	4.0	7	277
Std. Dev.		**0.648**			

[a] Relative wind direction shown is the angle from a vector normal to the plane of the configuration.

Table 3-5. Moving Average of Calculated Methane Flux, CCF, Wind Speed, and Wind Direction for 01/22/04 Downwind VRPM Survey (Collected with OP-FTIR).

Cycles	CCF	Flux (g/s)	Wind Speed (m/s)	Relative Wind Dir.[a] (deg)	Absolute Wind Dir. (deg from North)
1 to 3	0.962	17	4.4	25	290
2 to 4	0.958	20	4.5	28	293
5 to 7	0.892	17	4.3	17	282

continued

6 to 8	0.804	18	4.2	22	287
7 to 9	0.908	13	4.0	15	280
8 to 10	0.894	13	3.8	13	278
9 to 11	0.910	16	4.2	12	277
Std. Dev.		**2.42**			

[a] Relative wind direction shown is the angle from a vector normal to the plane of the configuration.

Figures 3-7 and 3-8 present the reconstructed methane plume from the upwind and downwind 22 January VRPM survey, respectively. Contour lines give methane concentrations (in parts per million) above ambient background concentration. The average calculated methane flux was 20 g/s for the upwind survey and 18 g/s for the downwind survey.

The shape of the plume from the upwind VRPM survey is not well developed vertically, suggesting that a methane hot spot may have been located upwind, close to the upwind VRPM plane. This finding is consistent with the other upwind VRPM surveys conducted during this campaign along the western boundary of the site.

The average methane flux during the upwind VRPM survey (20 g/s) was higher than the average flux measured during the downwind VRPM survey (18 g/s). This is probably due to reasons similar to those discussed in Section 3.2.2. The prevailing northwesterly winds observed during the survey probably carried most of the emissions from the suspected upwind methane hot spot through the upwind VRPM configuration. However, the prevailing winds again caused most of the emissions from this hot spot to be carried outside of the much shorter downwind VRPM configuration. Therefore, the flux measurements from the downwind VRPM survey may have been only slightly influenced by emissions from the suspected hot spot upwind of the site. The flux measured from the downwind survey is therefore primarily due to emissions from the methane hot spot found near the center of the site during the HRPM survey (see Figure 3-2).

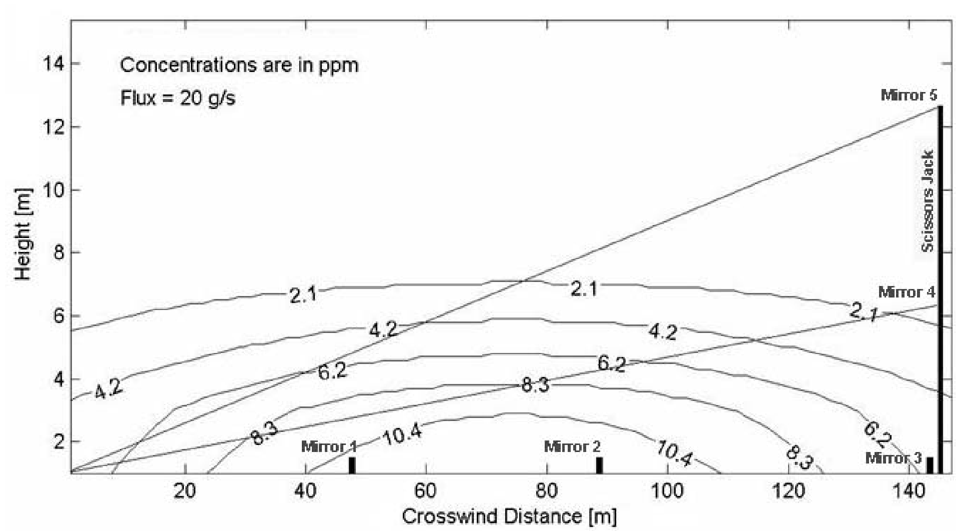

Figure 3-7. Average Reconstructed Methane Plume from the 01/22/04 Upwind VRPM Survey.

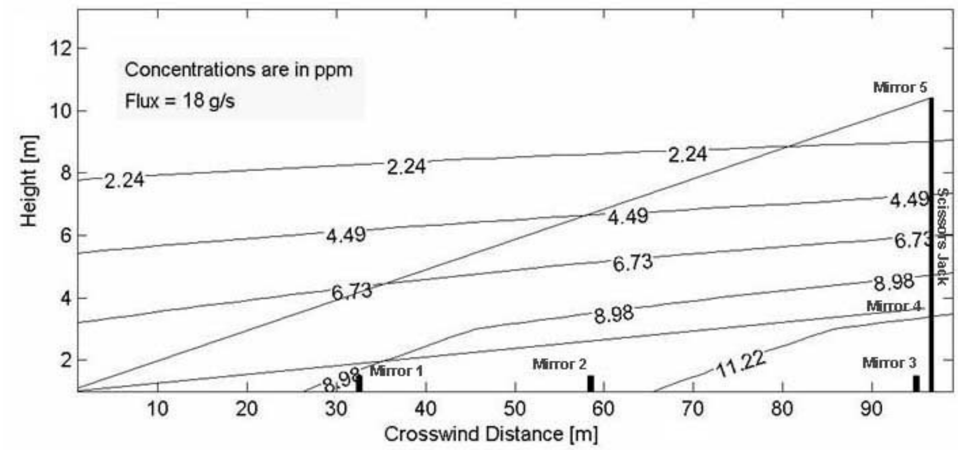

Figure 3-8. Average Reconstructed Methane Plume from the 01/22/04 Downwind VRPM Survey.

3.3 Results from the Single-Path Measurement during Leachate Pump Operation

During the afternoon of 21 January, leachate was being pumped from a holding pond adjacent to the site through a hose extending diagonally across the surface of the survey area. One single-path measurement was taken with the OP-FTIR to determine the emissions coming from the hose, and the path-averaged methane concentration was 57 ppm with a range of 32 to 94 ppm. These levels are approximately twice as high as concentrations found along comparable paths that can be derived from the HRPM surface data collected on the same day (see Figure 2-6) while the leachate pump was not operating.

3.4 VOC and Ammonia Results

All data sets from the HRPM and VRPM surveys were searched for the presence of VOCs and ammonia, and the analysis did detect the presence of ammonia and methanol at the site. However, levels of measured methanol were close to the detection limits of the instrument. Methanol was detected only during the 21 January single-path measurements conducted while the leachate pump was operating. Table 3-6 presents the range of measured ammonia and methanol concentrations and the minimum detection level (MDL) of the OP-FTIR instrument for each compound. See Section 1.3 for more information on the calculation of the MDL.

Table 3-6. Average Ammonia and Methanol Concentrations Measured.

Data Set	Compound	Range of Measured Concentration (ppb)	MDL (ppb)
1/20/04 VRPM Upwind Survey	Ammonia	2.8 to 22	2.0
1/21/04 VRPM Downwind Survey	Ammonia	5.0 to 27	3.4
1/21/04 VRPM Single-Path Leachate Path Survey	Ammonia	3.0 to 8.9	1.9
1/21/04 VRPM Single-Path Leachate Path Survey	Methanol	11	9.3
1/22/04 VRPM Upwind Survey	Ammonia	4.4 to 37	4.1
1/22/04 HRPM Morning Survey	Ammonia	6.3 to 25	2.8
1/22/04 HRPM Afternoon Survey	Ammonia	4.8 to 28	3.2

Chapter 4
Conclusion

This report presents the results from a field campaign conducted in January 2004 at the Three Rivers Solid Waste Technology Center Landfill, located near Aiken, SC. The study used measurements from ORS instruments and the ORS-RPM method to characterize fugitive emissions of methane and VOCs from the site.

HRPM surveys conducted on 21 and 22 January detected the presence of a methane hot spot near the center of the site. The peak concentration of this hot spot varied from over 26 ppm to over 48 ppm above ambient background concentrations.

A HRPM survey was conducted on the afternoon of 22 January while leachate was being pumped from a small holding pond in the southeast corner of the site to another small holding pond in the northwest corner of the site. This HRPM survey detected an additional methane hot spot near the site's northwest corner that had concentrations greater than 23 ppm above ambient background levels. This hot spot is probably associated with emissions from the leachate being pumped to the holding pond located in the northwest corner of the cell.

VRPM surveys were done at the site on each day of the field campaign. During each survey, one vertical configuration served as the upwind measurement, and the other served as the downwind measurement, depending on the prevailing wind direction. The use of an upwind VRPM configuration allowed for the calculation of an upwind flux value. Table 4-1 presents the calculated methane fluxes from each survey.

Table 4-1. Average Calculated Methane Fluxes Found During the Upwind and Downwind VRPM Surveys.

VRPM Survey	Calculated Methane Flux (g/s)	
	Upwind (Western)	Downwind Eastern
20 January 2004	15	N/A[a]
21 January 2004	14	10[b]
22 January 2004	20	18[b]

[a] Downwind methane flux data from the 01/20/04 VRPM survey is not available due to software problems in the field.

[b] Calculated downwind methane flux values are lower that the corresponding upwind values because the entire methane plume was not captured by the downwind VRPM configuration.

The results of the VRPM surveys suggest that a methane hot spot may have been located directly upwind of the upwind VRPM configurations, on the western side of the top surface. The highest upwind methane flux value (20 g/s) occurred on 22 January. The observed wind speeds on this day were almost twice as high as those observed on 20 January (the prevailing wind direction on 20 January was comparable to the wind direction on 22 January), which may have caused increased emissions from the upwind hot spot.

The downwind average methane flux values from 21 and 22 January are probably lower than the corresponding upwind values because the prevailing winds at the time of the surveys carried a large portion of the plume from the upwind hot spot outside of the much shorter downwind VRPM configurations.

The location of the plumes in each of the VRPM maps was very consistent with the prevailing wind direction during each survey. On 20 and 22 January, the west-northwesterly winds carried the plume from the upwind hot spot through the center of the upwind VRPM configurations. The west-northwesterly winds of 22 January carried the plume from the hot spot near the center of the site through the southern portion of the downwind VRPM configuration. On 21 January, the southwesterly winds carried the plumes from the upwind hot spot and hot spot near the center of the site through the northern portion of the upwind and downwind VRPM configuration, respectively.

The data sets from the HRPM and VRPM surveys were searched for the presence of VOCs and ammonia, and the analysis did detect ammonia and methanol at the site. The measured ammonia concentrations ranged from 2.8 to 37 ppm. Methanol was detected only during the 21 January single-path measurements conducted while the leachate pump was operating. The measured methanol concentration was 11 ppm, which was close to the detection limits of the OP-FTIR instrument.

Chapter 5
Quality Assurance/Quality Control

5.1 Equipment Calibration

As stated in the ECPD Optical Remote Sensing Facility Manual (U.S. EPA, 2004), all equipment is calibrated annually or cal-checked as part of standard operating procedures. Certificates of calibration are kept on file. Maintenance records are kept for any equipment adjustments or repairs in bound project notebooks that include the data and description of maintenance performed. Instrument calibration procedures and frequency are listed in Table 5-1 and further described in the text.

As part of the preparation for this project, a Category III Quality Assurance Project Plan (QAPP) was prepared and approved for each separate field campaign. In addition, standard operating procedures were in place during the field campaign.

Table 5-1. Instrumentation Calibration Frequency and Description.

Instrument	Measurement	Calibration Date	Calibration Detail
R.M. Young Wind Monitor	Wind Speed in mi/h	Calibrated by Manufacturer	Calibrated by Manufacturer
R.M. Young Wind Monitor	Wind direction in deg from North	Calibrated by Manufacturer	Calibrated by Manufacturer
Topcon Model GTS-211D Theodolite	Distance	1 May 2003	Calibration of Distance: Actual Distance = 50 ft Measured Distance = 50.6 and 50.5 ft
Topcon Model GTS-211D Theodolite	Angle	21 May 2003	Calibration of Angle: Actual Angle = 360° Measured Angle = 359°41′18″ and 359°59′55″

5.2 Assessment of DQI Goals

The critical measurements associated with this project and the established data quality indicator (DQI) goals in terms of accuracy, precision, and completeness are listed in Table 5-2. More information on the procedures used to assess DQI goals can be found in Section 10 of the ECPD Optical Remote Sensing Facility Manual (U.S. EPA, 2004).

Table 5-2. DQI Goals for Instrumentation.

Measurement	Analysis Method	Accuracy	Precision	Completeness
Analyte PIC	OP-FTIR: Nitrous Oxide Concentrations	±25%/15%/10%[a]	±10%	90%
Ambient Wind Speed	Met. heads side-by-side comparison in the field	±1 m/s	±1 m/s	90%
Ambient Wind Direction	Met. heads side-by-side comparison in the field	±10°	±10°	90%
Distance	Theodolite	±1 m	±1 m	100%

[a] The accuracy acceptance criterion of ±25% is for path lengths of less than 50m, ±15% is for path lengths between 50 and 100m, and ±10% is for path lengths greater than 100m.

5.2.1 DQI Check for Analyte PIC Measurement

The precision and accuracy of the analyte path-integrated concentration (PIC) measurements was assessed by analyzing the measured nitrous oxide (N_2O) concentrations in the atmosphere. A typical background atmospheric concentration for N_2O is about 315 ppb. This value may fluctuate due to seasonal variations in N_2O concentrations or elevation of the site.

The precision of the analyte PIC measurements was evaluated by calculating the relative standard deviation of each data subset. A subset is defined as the data collected along one particular path length during one particular survey in one survey sub-area. The number of data points in a data subset depends on the number of cycles used in a particular survey.

The accuracy of the analyte PIC measurements was evaluated by comparing the calculated N_2O concentrations from each data subsets to the background value of 315 ppb. The number of calculated N_2O concentrations that failed to meet the DQI accuracy criterion in each data subset was recorded.

Overall, 43 data subsets were analyzed from this field campaign. Based on the DQI criterion set forth for precision of ±10%, each of the 43 data subsets were found to be acceptable. The range of calculated relative standard deviations for the data subsets from this field campaign was 1.1 to 6.1 ppbm, which represents 0.35% to 1.9% RSD.

Each data point (calculated N_2O concentration) in the 43 data subsets were analyzed to assess whether or not it met the DQI criterion for accuracy of ±25% (315 ± 79 ppb) for path lengths less than 50 meters, ±15% (315 ± 47 ppb) for path lengths between 50 and 100 meters, and ±10% (315 ± 32 ppb) for path lengths greater than 100 meters. A total of 306 data points were analyzed, and 294 of the points met the DQI criteria for accuracy for a completeness of 96%.

5.2.2 DQI Checks for Ambient Wind Speed and Wind Direction Measurements

Section 10 of the ECPD Optical Remote Sensing Facility Manual (U.S. EPA, 2004) states that the DQI goals for precision and accuracy of the R.M. Young meteorological heads are assessed by collecting meteorological data for 10 min with the two heads set side-by side. This was not done prior to the current field campaign because this DQI procedure had not been implemented at the time of the study. However, checks for agreement of the wind speed and wind direction measured from the two heads (at heights of 2 m and 10 m) were done in the field during data collection. Although it is true that some variability in the parameters measured at both levels should be expected, this is a good first-step check for assessing the performance of the instruments. Another check is done in the field by comparing the measured wind direction to the forecasted wind direction for that particular day.

5.2.3 DQI Check for Precision and Accuracy of Theodolite Measurements

Although calibration of this instrument did not occur immediately prior to the current field campaign, the theodolite was originally calibrated by the manufacturer prior to being received by the U.S. EPA. Additionally, there are several internal checks in the theodolite software that prevent data collection from occurring if the instrument is not properly aligned on the object being measured or if the instrument has not been balanced correctly. When this occurs, it is necessary to reinitialize the instrument to collect data.

DQI checks were performed on the theodolite at a field site near Chapel Hill, NC, prior to the current field campaign. The calibration of distance measurement was done using a tape measure to compare the actual distance to the measured distance. This check was duplicated to test the precision of this measurement. The actual distance measured was 15.2m. The measured distance during the first test was 15.4m, and the measured distance during the second test was 15.4m. The results indicate the accuracy (1.3% bias for test one and two) and precision (0% RSD) of the distance measurement fell well within the DQI goals.

The check to test the precision and accuracy of the angle measurement was done by placing two mirror targets approximately 180 degrees apart. The theodolite was placed in the middle of the imaginary circle formed by the two mirrors. The actual angle was 360°. The angle measured during the first test was 359°41′18″, and the angle measured during the second test was 359°59′55″. The results indicate the accuracy and precision of the angle measurement fell well within the DQI goals.

5.3 QC Checks of OP-FTIR Instrument Performance

Several checks should be performed on the OP-FTIR instrumentation prior to deployment to the field, and during the duration of the field campaign. More information on these checks can be found in MOP 6802 and 6807 of U.S. EPA, 2004. At the time of the current field campaign, the procedures and schedule of QC checks were still being developed. Consequently, only a select set of checks were performed on both OP-FTIR instruments prior to deployment and during the field campaign.

Prior to deployment (15 January), the single beam ratio, baseline stability, electronic noise, saturation, linearity, and random baseline noise tests were performed on the IMACC OP-FTIR instrument, and the single beam ratio, signal-to-noise, ZPD stability, and saturation tests were performed on the Midac instrument. The results of the tests indicated that both instruments were operating within the acceptable criteria range.

On 20 January 2004, the single beam ratio, saturation, electronic noise, linearity, and random baseline noise tests were performed on both OP-FTIR instruments. The results of these tests indicated that the instruments were operating within the acceptable criteria range.

In addition to the QC checks performed on the OP-FTIR, the quality of the instrument signal (interferogram) was checked constantly during the field campaign. This was done by ensuring that the intensity of the signal is at least five times the intensity of the stray light signal (the stray light signal is collected as background data prior to actual data collection and measures internal stray light from the instrument itself). In addition to checking the strength of the signal, checks were done constantly in the field to ensure that the data were being collected and stored to the data collection computer. During the campaign, a member of the field team constantly monitored the data collection computer to make sure these checks were completed.

5.4 Validation of Concentration Data Collected with the OP-FTIR

During the analysis of the OP-FTIR data, a validation procedure was performed to aid in identifying the presence of ammonia and methanol in the dataset. This validation procedure involves visually comparing an example of the measured spectra to a laboratory-measured reference spectrum.

Figure 5-1 shows an example of a validation done using a spectrum collected during the 21 January single-path measurements conducted while the leachate pump was operating. Ammonia and methanol were detected in this particular spectrum. The ammonia and methanol features can be seen in the measured field spectrum (blue trace). Classical least squares (CLS) analysis performed on this spectrum resulted in determinations of 10.6±4.7 ppb of methanol, and 8.86±0.93 ppb of ammonia. The uncertainty value is equal to three times the standard error in the regression fit of the measured spectrum to a calibrated reference spectrum, propagated to the concentration determination.

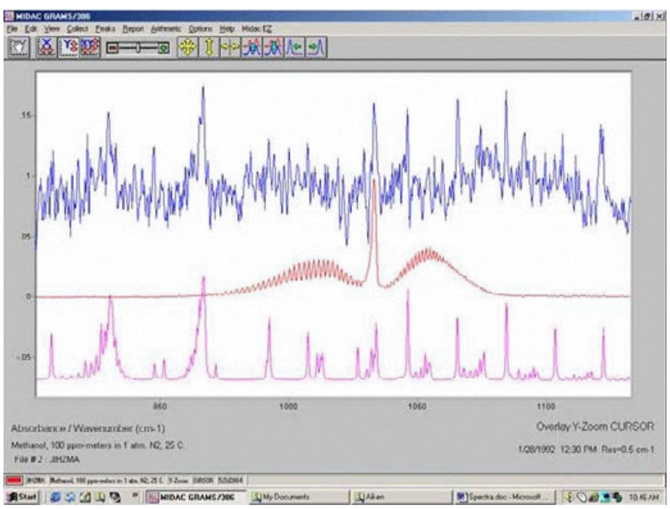

Figure 5-1. Comparison of a spectrum measured at the site (top trace) to the reference spectra of methanol (middle) and ammonia (bottom).

5.5 Internal Audit of Data Input Files

An internal audit was performed by the ARCADIS Field Team Leader on a sample of approximately 10% of the data from the field campaign. The audit investigated the accuracy of the input files used in running the RPM programs. The input files contain analyzed concentration data, mirror path lengths, and wind data. The results of this audit found no problems with the accuracy of the input files created.

5.6 OP-TDLAS Instrument

The development of calibration and standard operating procedures for the OP-TDLAS system has resulted in a major improvement in the data collection process. More information on collecting emissions measurements with the OP-TDLAS can be found in MOP 6811 of U.S. EPA, 2004.

The results of the current field campaign present methane concentrations measured with the OP-FTIR instrument and the OP-TDLAS system. In order to evaluate the comparability of measurements from the two instruments, an experiment was conducted during this field campaign to compare methane concentrations measured with the OP-TDLAS system and the IMACC OP-FTIR. The two instruments were deployed side-by-side at a location near the western boundary of the site, and aimed at an identical mirror located at a distance of 89 m. Methane concentration data were collected with each instrument for a period of 30 min. The OP-FTIR collected data at the same resolution (0.5 cm^{-1}) used in the current field campaign. Figure 5-2 shows that methane concentrations measured with the OP-TDLAS were slightly higher (3%) than concentrations measured with the OP-FTIR instrument. The results of this experiment show that the methane concentration measurements made from the OP-FTIR and OP-TDLAS instruments can be used to compare upwind and downwind data collected during this study.

5.7 Difficulties Encountered

During the course of the field campaign, the project encountered some difficulties. These included software problems with the scanner used to control the Midac OP-FTIR, difficulty in precisely time synchronizing the data collected from both VRPM configurations, and geographic barriers at the site that limited the sizes of the configurations used in the study.

On 20 January, the Midac OP-FTIR instrument was

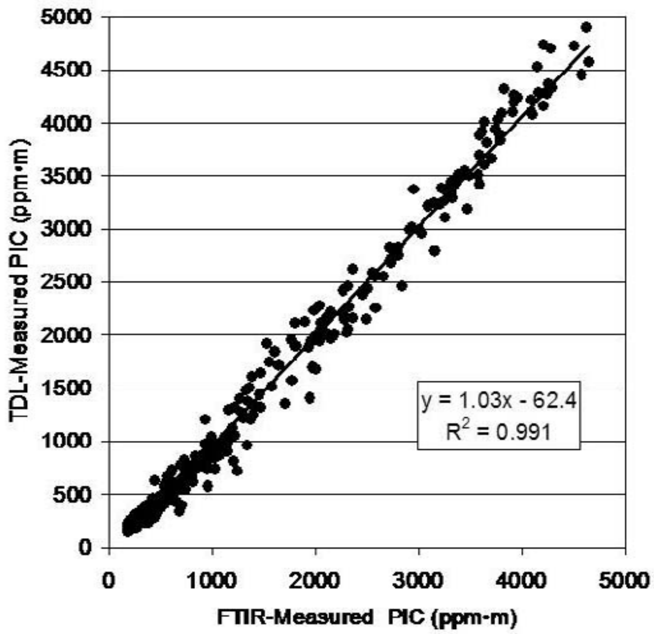

Figure 5-2. Comparison of Methane Concentrations Measured with the OP-TDLAS and OP-FTIR Instruments.

set up on the downwind side of the site. However, problems with the software used to control the scanner used with this instrument prevented downwind flux data from being collected on this day. Software problems continued with this instrument, and the OP-TDLAS instrument was needed to collect flux data for the duration of the project.

Another problem encountered was difficulty in precisely time synchronizing the data collected from the upwind and downwind VRPM configurations. Although the internal clocks on the data collection computers (used in the two VRPM configurations) were synchronized before data collection began, it was difficult to perfectly synchronize the starting and ending times of the data loops due to differences in the initialization and data collection times of the OP-TDLAS and OP-FTIR instruments. This problem made it difficult to compare short-term temporal variations in the upwind and downwind flux values collected during the VRPM surveys.

The geographical features of the site limited the size and location of the configurations used for data collection. The surface of the site along the eastern boundary was extremely uneven. This limited the distance of the VRPM configuration on the eastern side of the site to 95 m, which was much shorter than the VRPM configuration on the western side of the site (145 m). In cases where the winds were not close to perpendicular to the VRPM configurations, the shorter VRPM configuration along the eastern boundary of the survey area may not have captured the entire methane plume from the survey area. We suspect that this limitation contributed to the fact that the upwind flux values were sometimes greater than the downwind flux values. This problem could have been overcome if it had been possible to collect data for additional days when the prevailing wind direction had an eastern component (the longer western boundary would have become the downwind vertical plane in this case).

Despite these difficulties, the project was successful in producing surface methane concentration contour maps, and isolated methane flux values, especially from the western slope of the survey area (which were relatively consistent throughout the duration of the campaign).

Chapter 6
References

ASTM, 1999. American Society for Testing and Materials Standard Practice E1982-98, *Standard Practice for Open-Path Fourier Transform Infrared (OP/FT-IR) Monitoring of Gases and Vapors in Air*; March.

Hashmonay, R.A., M.G. Yost, D.B. Harris, and E.L. Thompson, 1998. Simulation study for gaseous fluxes from an area source using computed tomography and optical remote sensing, in *SPIE*, The International Society for Optical Engineering, Bellingham, WA, 3534, 405–410.

Hashmonay, R.A., M.G. Yost, and C. Wu, 1999. Computed tomography of air pollutants using radial scanning path-integrated optical remote sensing, *Atmos. Environ*., 33, 267–274.

Hashmonay, R.A., and M.G. Yost, 1999. Innovative approach for estimating fugitive gaseous fluxes using computed tomography and remote optical sensing techniques, *J. Air Waste Manage. Assoc*., 49, 966–972.

Hashmonay, R.A., D.F. Natschke, K.Wagoner, D.B. Harris, E.L.Thompson, and M.G. Yost, 2001. Field evaluation of a method for estimating gaseous fluxes from area sources using open-path Fourier transform infrared, *Environ. Sci. Technol*., 35, 2309–2313.

Hashmonay, R.A., K. Wagoner, D.F. Natschke, D.B. Harris, and E.L. Thompson, 2002. Radial computed tomography of air contaminants using optical remote sensing, in *Proceedings of the AWMA 95th Annual Conference and Exhibition*, VIP-110, Air & Waste Management Association, Pittsburgh, PA.

Platt, U., 1994. Differential optical absorption spectroscopy (DOAS), in *Air Monitoring by Spectroscopic Techniques, Chemical Analysis Series*, Vol. 127, John Wiley & Sons, Inc. pp. 27–84.

Wu, C., M.G. Yost, R.A. Hashmonay, and D.Y. Park, 1999. Experimental evaluation of a radial beam geometry for mapping air pollutants using optical remote sensing and computed tomography, *Atmos. Environ*., 33, 4709–4716,.

U.S. EPA, 1999. Compendium Method TO-16: Long-Path Open-Path Fourier Transform Infrared Monitoring of Atmospheric Gases; EPA-625/R-96/101b (NTIS PB99-172355), U.S. Environmental Protection Agency, Center for Environmental Research Information-Office of Research and Development: Cincinnati, Ohio, January.

U.S. EPA, 2004. ECPD Optical Remote Sensing Facility Manual, EPA-600/Q-04/088, National Risk Management Research Laboratory, Air Pollution Prevention and Control Division, Research Triangle Park, NC, August.

Appendix A
OP-FTIR Mirror Coordinates

Table A-1. Distance and Angular Coordinates of Mirrors Used in the 01/20/04 Upwind VRPM Survey.

Mirror Number	Distance (m)	Horizontal Angle from North (deg)	Vertical Angle[a] (deg)
1	48.2	184	0
2	89.2	180	0
3	144	179	0
4	145	178	2
5	146	177	5

[a] Vertical angle shown is the angle from horizontal (positive values indicate elevation from the horizontal, negative values indicate descent from the horizontal).

Table A-2. Distance and Angular Coordinates of Mirrors Used in the 01/20/04 Downwind VRPM Survey.

Mirror Number	Distance (m)	Horizontal Angle from North (deg)	Vertical Angle[a] (deg)
1	45.0	184	0
2	93.4	187	0
3	94.6	186	4

[a] Vertical angle shown is the angle from horizontal (positive values indicate elevation from the horizontal, negative values indicate descent from the horizontal).

Table A-3. Distance and Angular Coordinates of Mirrors Used in the 01/21/04 Upwind VRPM Survey.

Mirror Number	Distance (m)	Horizontal Angle from North (deg)	Vertical Angle[a] (deg)
1	32.6	182	0
2	62.3	184	0
3	94.4	185	0
4	94.9	184	1
5	95.6	185	5

[a] Vertical angle shown is the angle from horizontal (positive values indicate elevation from the horizontal, negative values indicate descent from the horizontal).

Table A-4. Distance and Angular Coordinates of Mirrors Used in the 01/21/04 Downwind VRPM Survey.

Mirror Number	Distance (m)	Horizontal Angle from North (deg)	Vertical Angle[a] (deg)
1	48.2	184	0
2	89.2	180	0
3	144	179	0
4	145	178	2
5	146	177	5

[a] Vertical angle shown is the angle from horizontal (positive values indicate elevation from the horizontal, negative values indicate descent from the horizontal).

Table A-5. Distance and Angular Coordinates of Mirrors Used in the 01/21/04 HRPM Survey.

Mirror Number	Distance (m)	Horizontal Angle from North (deg)
1	59.6	109
2	42.7	119
3	89.1	137
4	39.0	150
5	84.1	151
6	118	152
7	113	161
8	73.9	168
9	111	170

Table A-6. Distance and Angular Coordinates of Mirrors Used in the 01/22/04 HRPM Survey.

Mirror Number	Distance (m)	Horizontal Angle from North (deg)
1	107	187
2	69.1	191
3	117	199
4	120	209
5	39.0	208
6	77.3	211
7	82.3	223
8	45.2	236
9	58.5	253

Table A-7. Distance and Angular Coordinates of Mirrors Used in the 01/22/04 Downwind VRPM Survey.

Mirror Number	Distance (m)	Horizontal Angle from North (deg)	Vertical Angle[a] (deg)
1	32.6	173	0
2	58.5	175	0
3	94.9	170	0
4	95.9	169	2
5	96.6	169	6

[a] Vertical angle shown is the angle from horizontal (positive values indicate elevation from the horizontal, negative values indicate descent from the horizontal).

Appendix B
OP-TDLAS Configuration Path Lengths

Table B-1. Distance and Angular Coordinates of Mirrors Used in the OP-TDLAS Configuration.

Mirror Number	Distance (m)	Horizontal Angle from North (deg)	Vertical Angle[a] (deg)
1	47.7	184	0
2	88.5	181	0
3	144	179	0
4	145	179	3
5	146	177	5

[a] Vertical angle shown is the angle from horizontal (positive values indicate elevation from the horizontal, negative values indicate descent from the horizontal).

Appendix C
Methane Concentrations

Table C-1. Methane Concentrations (in PPM) found during the 01/20/04 Upwind VRPM Survey.

Cycle	Mirror Number				
	1	2	3	4	5
1	23.5	24.4	19.7	11.3	11.7
2	17.0	16.3	22.3	14.1	8.97
3	8.90	18.2	14.8	8.6	7.05
4	5.56	16.1	25.9	13.6	7.47
5	18.2	22.2	30.2	9.7	11.3
6	14.1	14.3	16.2	10.3	14.9
7	25.1	26.1	22.5	12.2	9.56
8	34.3	25.0	23.3	15.7	8.05
9	15.0	26.6	26.6	14.7	10.5
10	20.3	34.7	24.4	21.3	22.0
11	29.6	32.7	36.8	16.1	14.4
12	42.1	30.0	22.6	15.4	7.96

Table C-2. Methane Concentrations (in PPM) found during the 01/21/04 Upwind VRPM Survey.

Cycle	Mirror Number				
	1	2	3	4	5
1	28.8	15.8	9.61	7.38	7.21
2	8.81	5.76	4.32	4.04	4.92
3	6.30	5.90	6.55	7.10	3.35
4	6.52	4.67	4.13	4.36	4.70
5	9.27	6.75	6.33	6.88	5.86
6	10.1	10.5	12.4	8.47	5.71
7	13.1	7.33	5.91	7.08	5.64
8	8.25	4.73	4.00	4.44	3.71
9	6.79	5.89	3.71	3.77	4.69
10	6.81	5.81	6.70	4.00	4.20
11	5.79	4.98	3.62	3.00	2.94
12	12.1	10.4	8.43	6.85	3.82
13	12.8	10.4	11.0	6.84	4.12
14	7.54	15.0	13.1	5.94	5.16
15	15.1	8.40	8.60	4.94	7.69
16	31.1	20.4	11.8	12.7	11.0
17	19.0	14.6	7.21	7.83	8.36
18	33.3	12.3	8.96	5.49	4.76
19	8.91	8.65	9.01	5.95	4.38
20	18.9	7.65	12.7	6.01	5.24
21	12.2	11.2	6.69	4.27	9.20
22	23.0	23.1	14.8	12.6	6.43
23	32.3	20.7	18.9	10.4	8.98
24	29.8	21.4	16.7	10.3	12.3
25	32.6	17.9	11.2	6.71	5.82
26	21.5	15.7	9.10	11.8	5.32
27	12.6	7.64	19.3	9.90	8.18
28	19.8	16.0	13.0	7.47	6.42
29	15.9	14.2	9.68	6.57	6.33
30	24.9	16.1	14.2	8.84	9.37

Table C-3. Methane Concentrations (in PPM) found during the 01/21/04 Downwind VRPM Survey.

Cycle	Mirror Number				
	1	2	3	4	5
1	17.4	20.9	16.4	14.5	10.5
2	18.2	23.7	13.9	10.3	10.6
3	12.2	9.36	14.2	11.3	9.06
4	6.86	13.5	21.5	12.4	15.6
5	25.1	20.5	17.8	15.2	10.2
6	6.36	21.9	15.7	16.0	10.9
7	19.8	26.0	15.4	9.04	8.61
8	10.2	13.4	16.7	15.8	15.3
9	29.7	25.2	12.9	8.33	7.73
10	15.8	28.4	21.7	14.1	7.06
11	16.6	9.37	16.0	11.9	5.67
12	12.9	19.9	14.4	16.0	16.2
13	30.6	25.9	14.5	8.22	7.58
14	15.5	15.7	14.7	10.5	8.13
15	20.9	12.7	16.2	13.4	13.1
16	14.7	10.2	19.5	9.88	13.2
17	20.9	28.0	22.0	15.8	11.1
18	26.3	12.5	10.8	18.1	10.8
19	24.9	13.3	20.7	17.1	3.23
20	16.4	21.8	25.0	17.4	9.90
21	18.6	20.6	22.8	10.0	7.43
22	34.7	24.5	11.6	11.8	7.88
23	29.5	30.5	17.1	11.2	9.37
24	39.6	23.1	14.8	18.9	13.4

Table C-4. Methane Concentrations (in PPM) found during the 01/21/04 HRPM Survey.

Cycle	Mirror Number								
	1	2	3	4	5	6	7	8	9
1	12.2	20.6	29.4	15.1	34.5	30.5	22.5	23.8	19.5
2	19.7	22.3	24.0	8.50	35.1	20.0	26.6	17.2	

Table C-5. Methane Concentrations (in PPM) found during the 01/22/04 Downwind VRPM Survey.

Cycle	Mirror Number				
	1	2	3	4	5
1	8.48	10.01	12.80	10.65	6.78
2	11.77	9.86	11.56	9.04	5.15
3	10.36	9.03	11.48	8.39	7.17
4	9.54	11.16	10.83	11.32	9.80
5	18.01	17.60	13.18	8.60	6.69
6	9.53	9.97	9.23	8.89	5.69
7	9.34	13.07	15.15	10.29	9.54
8	11.78	9.48	14.27	6.47	6.25
9	11.68	13.42	15.82	8.79	4.58
10	6.58	13.65	15.44	10.13	9.89
11	17.05	11.29	13.13	8.97	6.52

Table C-6. Methane Concentrations (in PPM) found during the 01/22/04 HRPM Survey.

Cycle	Mirror Number								
	1	2	3	4	5	6	7	8	9
1	22.3	35.9	27.3	24.1	15.0	32.7	15.8	13.5	22.6
2	23.9	16.6	25.4	24.4	14.5	28.6	13.3	20.5	16.9
3	20.9	22.7	25.7	21.5	14.6	24.8	11.2	13.4	16.5
4	19.5	21.4	29.4	24.8	13.9	28.0	16.7	22.8	22.1
5	25.4	19.1	30.0	24.4	12.4	24.3	21.4	16.7	26.0
6	24.3	23.9	26.8	20.4	14.7	17.0	13.2	22.5	13.9
7	20.4	17.9	19.3	19.6	13.2	18.2	14.4	9.95	17.2
8	19.5	15.0	16.8	18.7	9.14	17.0	13.1	11.6	18.2
9	22.9	21.6	27.9	24.6	21.5	19.3	13.4	14.8	20.4
10	22.0	20.7	21.6	22.7	23.4	24.8	9.90	10.3	9.34
11	18.2	12.4	21.7	19.1	10.3	28.1	11.1	15.0	18.1